Number of Tables: 2

# Effects of dipeptidyl peptidase 4 inhibition on inflammation in atherosclerosis: A $^{18}$F-fluorodeoxyglucose study of a mouse model of atherosclerosis and type 2 diabetes

Jenni Virta[a], Sanna Hellberg[a,b], Heidi Liljenbäck[a,c], Mia Ståhle[a], Johanna M. U. Silvola[a], Jenni Huusko[d], Mirva Söderström[e], Juhani Knuuti[a,f], Pirjo Nuutila[a,f,g], Seppo Ylä-Herttuala[d,h], Maria F. Gomez[i], Anne Roivainen[a,c,f], Antti Saraste[a,f,j]

[a]Turku PET Centre, University of Turku, Kiinamyllynkatu 4-8, FI-20520 Turku, Finland

[b]Department of Medicine, Karolinska Institutet, Akademiska stråket 1, SE-17164 Solna, Sweden

[c]Turku Center for Disease Modeling, University of Turku, Kiinamyllynkatu 10, FI-20520 Turku, Finland

[d]A.I. Virtanen Institute for Molecular Sciences, University of Eastern Finland, Kuopio, Neulanniementie 2, FI-70210 Kuopio, Finland

[e]Department of Pathology, Turku University Hospital, Kiinamyllynkatu 10, FI-20520 Turku, Finland

[f]Turku PET Centre, Turku University Hospital, Kiinamyllynkatu 4-8, FI-20520 Turku, Finland

[g]Department of Endocrinology, Turku University Hospital, Kiinamyllynkatu 4-6, FI-20520 Turku, Finland

[h]Heart Center, Kuopio University Hospital, Puijonlaaksontie 2, FI-70210 Kuopio, Finland

[i]Department of Clinical Sciences, Lund University, Jan Waldenströms gata 35, SE-21428 Malmö, Sweden

[j]Heart Center, Turku University Hospital, Hämeentie 11, FI-20520 Turku, Finland

Correspondence: Antti Saraste

Turku PET Centre, Turku University Hospital, Kiinamyllynkatu 4-8, FI-20520 Turku, Finland.

Tel: +35823130083; Fax: +35822318191; E-mail: antti.saraste@utu.fi

Word count: Abstract: 250 words, main text: 4038

Number of figures: 4 (color print required)

**Keywords**: atherosclerosis, type 2 diabetes, $^{18}$F-fluorodeoxyglucose, inflammation, linagliptin

**Abbreviations**

ApoB, apolipoprotein B; ApoE, apolipoprotein E; AUC, area under the curve; CVD, cardiovascular disease; DPP-4, Dipeptidyl peptidase 4; $^{18}$F-FDG, 2-deoxy-2-[$^{18}$F]-fluoro-*D*-glucose; GLP-1, glucagon-like peptide 1; GLP-1R, glucagon-like peptide 1 receptor; H&E, hematoxylin-eosin; HFD, high-fat diet; IGF-II, insulin-like growth factor II; IMT, intima-media thickness; iNOS, inducible nitric oxide synthase; Ldlr, low-density lipoprotein receptor; MRC-1, mannose-receptor C-type 1; oGTT, oral glucose tolerance test; NAFLD, non-alcoholic fatty liver disease; NAS, NAFLD score; PET, positron emission tomography; PSL/mm$^2$, photo-stimulated luminescence per square millimeter; ROI, region of interest; SUV, standardized uptake value; T2DM; type 2 diabetes mellitus; WAT, white adipose tissue

**Abstract**

*Background and aims*: Dipeptidyl peptidase 4 (DPP-4) inhibitors have anti-inflammatory and atheroprotective effects. We evaluated the effects of the DPP-4 inhibitor linagliptin on atherosclerotic plaque and hepatic inflammation using histology and 2-deoxy-2-[$^{18}$F]-fluoro-*D*-glucose ($^{18}$F-FDG), a positron emission tomography tracer of inflammation, in a mouse model of hypercholesterolemia and type 2 diabetes.

*Methods*: *Igf2/Ldlr*$^{-/-}$*Apob*$^{100/100}$ mice were fed a high-fat diet (HFD) for 8 weeks and then randomly allocated to receive HFD (n = 14), or HFD with added linagliptin (n = 15) for additional 12 weeks. Five mice fed a chow diet were studied as an additional control. At the end of the study, glucose tolerance, aortic and liver uptake of $^{18}$F-FDG, and histology were studied.

*Results*: Mice in linagliptin and HFD groups had similar fasting glucose concentrations, but linagliptin improved glucose tolerance. Aortas of linagliptin and HFD groups showed advanced atherosclerotic plaques with no difference in the mean intima-to-media ratio or number of macrophages in the plaques. Autoradiography showed similar $^{18}$F-FDG uptake by atherosclerotic plaques in linagliptin and HFD groups (plaque-to-wall ratio: 1.7 ± 0.25 *vs* 1.6 ± 0.21; $p = 0.24$). In the liver, linagliptin reduced the histologic inflammation score but had no effect on $^{18}$F-FDG uptake. Compared with chow diet, uptake of $^{18}$F-FDG was similar in the aorta, but higher in the liver after HFD.

*Conclusions*: Linagliptin therapy improved glucose tolerance and reduced hepatic inflammation but had no effect on plaque burden or atherosclerotic inflammation, as determined by histology and $^{18}$F-FDG uptake, in atherosclerotic mice with type 2 diabetes.

## 1. Introduction

Diabetes is associated with a greater risk of atherosclerotic cardiovascular disease (CVD) and is common in patients with known CVD or those at risk of CVD. Various factors, including oxidative stress and the consequent activation of pro-inflammatory pathways, as well as greater cell proliferation in the arterial wall, contribute to more rapid progression of atherosclerosis in diabetes [1]. Dipeptidyl peptidase-4 (DPP-4) inhibitors and glucagon-like peptide-1 receptor (GLP-1R) agonists have been shown to prevent progression of atherosclerosis and cardiovascular complications in patients with type 2 diabetes mellitus (T2DM), but the underlying mechanisms are incompletely understood [2-4].

Experimental studies have shown that DPP-4 inhibition reduced the area of atherosclerotic lesions in both apolipoprotein E (*ApoE*)-deficient [5-6] and low-density lipoprotein receptor deficient ($Ldlr^{-/-}$) mice [7]. These effects were associated with a reduction in the accumulation of monocytes and macrophages in the vascular wall [5-7] as well as lower expression of pro-inflammatory mediators by macrophages [8]. In diet-induced obese *C57BL/6* mice, treatment with the DPP-4 inhibitor linagliptin has also been shown to alleviate hepatic steatosis and inflammation [9-10].

Positron emission tomography (PET) using the glucose analogue 2-deoxy-2-[$^{18}$F]-fluoro-*D*-glucose ($^{18}$F-FDG) enables non-invasive imaging of atherosclerotic plaque inflammation due to high glucose uptake by macrophages [11]. Studies have shown that the presence of impaired glucose tolerance [12], T2DM [12-14] and metabolic syndrome [15] increase the arterial uptake of $^{18}$F-FDG. Recent studies have supported a key role for activation of glucose metabolism to support inflammation and a high-risk phenotype of atherosclerotic plaques [16]. Thus, $^{18}$F-FDG-PET represents a translational tool to address effects of therapies on atherosclerotic plaque activity. We hypothesized that linagliptin therapy would reduce activity of glucose metabolism related to inflammation in atherosclerotic lesions and hepatic steatosis. We evaluated the effects of 3 months of

treatment with linagliptin on inflammation in atherosclerotic plaques and in the liver in a mouse model of atherosclerosis and T2DM, using uptake of the PET tracer $^{18}$F-FDG and histology.

## 2. Materials and methods

### *2.1. Animals and study design*

A total of 34 male diabetic, hypercholesterolemic mice overexpressing insulin-like growth factor II (*Igf2*) in pancreatic β-cells, deficient in low-density lipoprotein receptor (*Ldlr*), and expressing apolipoprotein B100 only (*Igf2/Ldlr*$^{-/-}$*/ApoB*$^{100/100}$) were used [17]. Twenty nine mice were initially fed a chow diet (9.1% of calories from fat, CRM [E], 801730; Special Diet Services, Essex, UK) for 2 months and then switched to a high-fat diet (HFD, 42% of calories from fat, 0.2% total cholesterol, TD 88137 mod; Ssniff Spezialdiäten GmbH, Soest, Germany) for a further 2 months. The mice were then randomly allocated to two groups: the HFD group (n = 14) continued to consume the high-fat diet, and the linagliptin group (n = 15) consumed a high-fat diet mixed with linagliptin (85 mg/kg of feed; Boehringer Ingelheim International GmbH, Ingelheim am Rhein, Germany) for 3 months. Five mice were fed a chow diet throughout the study period.

Oral glucose tolerance testing (oGTT) was performed at baseline, before the start of the intervention, and again at the end of the intervention (See Supplemental Data). The food consumption and body mass of the mice were monitored weekly.

To determine the effects of linagliptin on plasma DPP-4 activity and on active GLP-1 plasma concentration in *Igf2/Ldlr*$^{-/-}$*/ApoB*$^{100/100}$ mice, blood samples obtained from 15 mice after 12 weeks of linagliptin administration (~10 mg/kg/day in feed, based on a mean measured daily food intake of 3–4 g per mouse) and from 14 control mice were assayed, as previously described [18].

The experiments were approved by the National Animal Experiment Board in Finland and the Regional State Administrative Agency for Southern Finland, and they were carried out in accordance with the European Union directives on animal experimentation.

*2.2. $^{18}$F-FDG biodistribution and uptake by the aorta and liver*

After the intervention period, the mice were fasted for 2–4 h, anesthetized with isoflurane (1–2%) and kept on heating pads during their anesthesia. The mice were injected with 10 ± 0.23 MBq of $^{18}$F-FDG *via* tail vein catheters and then sacrificed by cardiac puncture and cervical dislocation 90 min post-injection. Blood glucose concentration was measured before the injection and at the time of sacrifice.

To assess the biodistribution of $^{18}$F-FDG, the thoracic aorta, liver, and other selected tissues were excised and weighed, and their total radioactivity content was measured using a gamma counter (Triathler 3″; Hidex, Turku, Finland). The results are expressed as standardized uptake values (SUV = [tissue radioactivity/tissue weight]/total injected radioactivity/mouse body mass) or target-to-background ratio ($SUV_{aorta}/SUV_{blood}$).

To assess $^{18}$F-FDG uptake, the aorta and a liver lobe from each mouse were embedded in OCT compound and frozen in dry-ice-cooled isopentane, and serial longitudinal sections of 20 and 8 µm were prepared. Digital autoradiography was performed as described previously [19]. The 20 µm sections were stained with hematoxylin-eosin (H&E) and aligned with the autoradiographs. Regions of interest (ROIs) were defined in the plaques and non-atherosclerotic vessel wall on the basis of the histology. In the liver, the ROI encompassed the entirety of the samples. The results are given as count density (photo-stimulated luminescence per square millimeter, PSL/mm$^2$), normalized for the injected dose of radioactivity per unit body mass and for the radioactive decay during exposure. The plaque-to-wall ratio was calculated for each mouse by dividing the mean PSL/mm$^2$ values for the plaque by the mean PSL/mm$^2$ for the non-atherosclerotic vessel wall.

*2.3. Histology and immunohistochemistry*

To assess plaque burden and inflammation, formalin-fixed, paraffin-embedded aortic roots were cut transversely into 6 µm serial sections at the level of coronary artery ostium and stained with modified Movat's pentachrome for histologic evaluation, or they were subjected to immunohistochemistry using a mouse anti-Mac-3 antibody to identify macrophages, an anti-mannose receptor C-type 1 antibody (MRC-1) to identify M1-polarized macrophages; or an anti-inducible nitric oxide synthase antibody (iNOS) to identify M2-polarized macrophages (Supplemental Data). Area of the intima and intimal areas positive for Mac-3, MRC-1, or iNOS were determined using ImageJ software (National Institutes of Health, Bethesda, MD, USA).

To evaluate liver histology, a formalin-fixed, paraffin-embedded lobe of the liver was cut into 4 µm sections and stained with H&E or van Gieson's stain. Features of NAFLD (steatosis, inflammation, ballooning, and fibrosis) were evaluated by two independent observers using the NAFLD activity scoring (NAS) scale [20] (Supplemental Data).

*2.4. Statistical methods*

The results are expressed as mean ± SD. Analyses were performed using IBM SPSS Statistics 25 (IBM Corp., Armonk, NY, USA). Normally distributed datasets were analyzed using Student's *t*-test for unpaired data to compare the differences between linagliptin and HFD group or HFD and chow group. Fisher's exact test was used to evaluate the NAFLD scores, and correlations were evaluated using Spearman's rho. Statistical significance was accepted when $p < 0.05$. The sample size used was based on the assumption of a mean $^{18}$F-FDG uptake by atherosclerotic plaques (plaque-to-wall ratio on autoradiography) of 1.95 ± 0.33 [21]. On this basis, 11 mice per group would be required to detect a 20% difference in uptake with 80% power and an alpha value of 0.05.

## 3. Results

### *3.1. General characteristics*

The general characteristics of the mice were similar between linagliptin and HFD groups (Table 1). Food consumption was 3.2 ± 0.31 g/day in linagliptin group, 3.1 ± 0.28 g/day in HFD group and 3.8 ± 0.2 g/day in chow group (HFD *vs.* chow; $p = 0.001$). This resulted in a mean intake of linagliptin of 7.7 ± 0.98 mg/kg/day. Total cholesterol level was higher in mice on HFD than chow diet. In a separate group of mice, linagliptin treatment lowered plasma DPP-4 activity by 83% compared with HFD mice (749 ± 127 *vs.* 4,488 ± 783 relative fluorescence units, respectively; $p < 0.001$). GLP-1 activity was 81% higher in linagliptin-treated mice than in HFD mice (16 ± 5.2 *vs.* 2.9 ± 2.3 pg/ml, respectively; $p < 0.001$).

### *3.2. Effect of linagliptin on glucose tolerance*

Before the intervention, oGTT showed no differences in glucose tolerance between the linagliptin and HFD (area under the curve $[AUC]_{0–120\ min}$ 2,033 ± 435 *vs.* 1,976 ± 419 mmol.min/l, respectively; $p = 0.72$) or HFD and chow groups ($AUC_{0–120\ min}$ 1,976 ± 419 *vs.* 2,339 ± 318 mmol·min/l; $p = 0.10$) (Fig. 1A and 1E).

At the end of the intervention, linagliptin group demonstrated better glucose tolerance compared to baseline ($AUC_{0–120\ min}$ 1,365 ± 313 mmol.min/l *vs.* 2,033 ± 435; $p < 0.001$), and HFD group ($AUC_{0–120\ min}$ 1,365 ± 313 *vs.* 1,720 ± 397 mmol.min/l; $p = 0.01$). There was no difference between HFD and chow group (Fig. 1C and 1E).

There were no significant differences between linagliptin and HFD group in whole blood insulin concentrations during the oGTT (Fig. 1B and 1D). However, in linagliptin group insulin concentrations were significantly increased at the end of the intervention compared to baseline ($AUC_{0–120\ min}$ 75 ± 14 *vs.* 143 ± 59 ng·min/ml; $p = 0.001$) (Fig. 1F).

*3.3. $^{18}$F-FDG uptake*

There was no difference in the aortic $^{18}$F-FDG uptake between linagliptin and HFD groups (SUV 1.0 ± 0.23 *vs*. 1.1 ± 0.27, $p = 0.74$; aorta-to-blood ratio 3.2 ± 0.78 *vs*. 3.0 ± 0.58, $p = 0.60$). Neither was there a difference between HFD and chow groups (SUV 1.1 ± 0.27 *vs.* 1.2 ± 0.60; $p = 0.54$; aorta-to-blood ratio 3.0 ± 0.58 *vs.* 2.5 ± 0.70; $p = 0.12$). $^{18}$F-FDG uptake by white adipose tissue was lower in linagliptin group than in HFD group (SUV 0.07 ± 0.02 *vs*. 0.10 ± 0.04, respectively; $p = 0.04$) (Supplemental Table 1).

Autoradiography was used to demonstrate the uptake of $^{18}$F-FDG into the vessel walls at the sites of atherosclerotic lesions (Fig. 2). There were no differences in $^{18}$F-FDG uptake by atherosclerotic lesions, the non-atherosclerotic vessel wall, or the liver between linagliptin and HFD group. Chow group had significantly lower hepatic $^{18}$F-FDG uptake compared to HFD group (93 ± 16 *vs*. 134 ± 36 PSL/mm$^2$; $p = 0.03$) (Table 2).

*3.4. Histologic evaluation*

The histology of the aortic root was evaluated, as shown in Fig. 3. The area of the intima was similar in linagliptin and HFD groups. Both groups showed lesions infiltrated with Mac-3-positive macrophages and had similar ratios of M1- and M2-polarized macrophages. Compared to HFD group, chow group had significantly smaller intimal area ($p < 0.001$), but the lesions were similarly infiltrated with Mac-3-positive macrophages (Table 2).

Liver histopathology was also evaluated from sections stained with H&E and van Gieson (Fig. 4A-C). Linagliptin-treated and HFD mice showed prominent steatosis, but linagliptin-treated mice had significantly less inflammation than HFD mice ($p = 0.04$). In addition, the number of ballooned cells was similar and there was minimal fibrosis in both groups. There were no differences between linagliptin-treated and HFD mice with respect to NAS or fibrosis. Mice showed less steatosis on chow diet than HFD ($p = 0.02$), but there were no differences in inflammation, NAS or fibrosis (Table

2). Finally, liver $^{18}$F-FDG uptake positively correlated with the degree of steatosis ($r_S$ = 0.45, $p$ = 0.007) and aortic $^{18}$F-FDG uptake ($r_S$ = 0.52, $p$ = 0.002), but not with the degree of inflammation ($r_S$ = 0.34, $p$ = 0.051).

## 4. Discussion

The present study shows that oral linagliptin treatment does not affect atherosclerotic plaque formation or inflammation in the atherosclerotic and diabetic *Igf2/Ldlr*$^{-/-}$*/ApoB*$^{100/100}$ mouse, as determined using aortic $^{18}$F-FDG uptake and histologic analysis of the severity of macrophage infiltration into the aortic sinus. However, linagliptin increased insulin secretion and ameliorated liver inflammation and glucose intolerance, showing that the mice responded to antidiabetic medication as expected.

In previous studies, the area of the atherosclerotic lesions was reduced by DPP-4 inhibition in *ApoE*-deficient mice [5-6,8] and *Ldlr*$^{-/-}$ mice [7]. Furthermore, the GLP-1R agonist exendin-4 has been shown to attenuate atherosclerosis in normoglycemic *ApoE*$^{-/-}$ mice [22]. Liraglutide showed beneficial effects in early-onset, mild atherosclerosis, although this effect was lost in late-onset severe atherosclerosis [23]. By contrast, another study of hyperglycemic *ApoE*$^{-/-}$ mice showed no anti-atherosclerotic effects of the GLP-1R agonist taspoglutide [24]. In the present study, we found only a tendency toward smaller atherosclerotic lesions in the linagliptin group. However, because the aortic root usually contains the most advanced lesions we cannot exclude the possibility that the lesions could have been reduced in size in other parts of the aorta.

The suppression of vascular inflammation has been proposed as a mechanism underlying the anti-atherosclerotic effect of DPP-4 inhibition. Ervinna *et al.* demonstrated a smaller area of Mac-2-positive macrophages in atherosclerotic lesions at the aortic sinus level of *ApoE*$^{-/-}$ mice after 16 weeks of treatment with the DPP-4 inhibitor anagliptin [6]. *In vitro*, anagliptin has been shown to reduce the expression of proinflammatory mediators in monocytes and macrophages in a dose-

dependent manner [6], and alogliptin has been shown to reduce monocyte migration [7]. In contrast to the results of these previous studies linagliptin treatment did not reduce the number of Mac-3-positive macrophages in our model. Furthermore, we have extended the previous studies by evaluating $^{18}$F-FDG uptake in the aorta. $^{18}$F-FDG-PET can be used to quantify inflammation in atherosclerotic lesions in a non-invasive and reproducible manner, because increases in $^{18}$F-FDG accumulation reflect higher glucose consumption by inflammatory cells [11,21,25,26]. Previous studies indicate that a metabolic marker like $^{18}$F-FDG uptake is sensitive to changes caused by short-term interventions, irrespective of alterations in plaque burden [25]. Here, linagliptin treatment did not reduce $^{18}$F-FDG uptake in the whole aorta (biodistribution) or in the atherosclerotic lesions (by autoradiography), implying that DDP-4 inhibition does not have significant impact on glucose metabolism related to inflammation in atherosclerotic lesions.

Linagliptin treatment appeared to reduce $^{18}$F-FDG uptake into white adipose tissue that is consistent with previous studies showing less severe inflammation in the adipose tissue of *Ldlr*$^{-/-}$ mice [7] or mice with diet-induced obesity [27-28], following DPP-4 inhibition.

DPP-4 inhibitors and GLP-1R agonists may have beneficial effects on NAFLD in patients with T2DM [29]. Linagliptin alleviated hepatic steatosis and inflammation in diabetic and non-diabetic mice fed a high-fat diet [9,27,30]. The modest effects observed in the present study may be explained by the relatively mild hepatic disease present in the model. Although previous studies have suggested $^{18}$F-FDG uptake in the liver of patients with NAFLD to reflect inflammation [31-32], we did not find a correlation between liver inflammation and $^{18}$F-FDG uptake. Instead, $^{18}$F-FDG uptake correlated with the degree of steatosis, consistent with previous studies [31,33].

There were a number of limitations to our study. The reasons for the insulin resistance in the mouse model used are not fully understood, and the model does not reproduce the full phenotype of T2DM in human patients, implying that our findings should be validated in clinical studies [34]. The study was powered to detect a 20% difference in $^{18}$F-FDG uptake at 80% probability [21,26].

However, even smaller differences might still be clinically significant during the progression of the disease over a longer period of time.

In conclusion, linagliptin improved glucose tolerance and reduced hepatic inflammation but had no effect on the uptake of the PET tracer $^{18}$F-FDG in the atherosclerotic aortae of mice with hypercholesterolemia and T2DM. These results are not consistent with a significant anti-inflammatory effect of DPP-4 inhibition in atherosclerotic lesions.

**Conflict of interest:** None.

**Financial support**

This study was conducted in the Finnish Centre of Excellence in Cardiovascular and Metabolic Diseases, which is supported by the Academy of Finland, University of Turku, Turku University Hospital, and Åbo Akademi University. The research was also supported by the Turku University Foundation, the Sigrid Jusélius Foundation, the Finnish Foundation for Cardiovascular Research, Jane and Aatos Erkko Foundation and the Innovative Medicines Initiative Joint Undertaking, under grant agreement no. 115006 (the SUMMIT consortium), which provides resources composed of a financial contribution from the European Union's Seventh Framework Program (FP/2007-2013) and generous contributions from European Federation of Pharmaceutical Industries and Associations companies. The funders had no role in the study design, the data collection and analysis, or the preparation of the manuscript. J.V. was financially supported by the Drug Research Doctoral Programme, University of Turku Graduate School.

**Author contributions**

J.V. contributed to the study design, organized the study, performed the animal experiments and plasma analyses, acquired and analyzed the data, and drafted the manuscript. H.L., S.H., and

M.ST. participated in the animal studies and data analyses. M.S. performed the histopathologic analysis. J.M.U.S. contributed to the study design. J.H., J.K., P.N., S.Y-H, A.R., A.S., and M.F.G. designed the study and made critical contributions to the drafting of the manuscript. All authors read and approved the final manuscript.

**Acknowledgements**

The authors thank Erica Nyman, Marja-Riitta Kajaala, Aake Honkaniemi and Reija Suomi for technical assistance and Timo Kattelus for preparing figures.

**References**

1. G. Pasterkamp, Methods of accelerated atherosclerosis in diabetic patients, Heart 99 (2013) 743-749.
2. M.A. Nauck, J.J. Meier, M.A. Cavender, M. Abd El Aziz, D.J. Drucker, Cardiovascular actions and clinical outcomes with glucagon-like peptide-1 receptor agonists and dipeptidyl peptidase-4 inhibitors, Circulation. 136 (2017) 849-870.
3. T. Mita, N. Katakami, H. Yoshii et al., Alogliptin, a dipeptidyl peptidase 4 inhibitor, prevents the progression of carotid atherosclerosis in patients with type 2 diabetes: the study of preventive effects of alogliptin on diabetic atherosclerosis (SPEAD-A), Diabetes Care 39 (2016) 139-148.
4. S. Ishikawa, M. Shimano, M. Watarai et al., Impact of sitagliptin on carotid intima-media thickness in patients with coronary artery disease and impaired glucose tolerance or mild diabetes mellitus, Am. J. Cardiol. 114 (2014) 384-388.
5. H.M. Salim, D. Fukuda, Y. Higashikuni et al., Dipeptidyl peptidase-4 inhibitor, linagliptin, ameliorates endothelial dysfunction and atherogenesis in normoglycemic apolipoprotein-E deficient mice, Vascul. Pharmacol. 79 (2016) 16-23.

6. N. Ervinna, T. Mita, E. Yasunari et al., Anagliptin, a DPP-4 inhibitor, suppresses proliferation of vascular smooth muscles and monocyte inflammatory reaction and attenuates atherosclerosis in male apo E-deficient mice, Endocrinology 154 (2013) 1260-1270.
7. Z. Shah, T. Kampfrath, J.A. Deiuliis et al., Long-term dipeptidyl-peptidase 4 inhibition reduces atherosclerosis and inflammation via effects on monocyte recruitment and chemotaxis, Circulation 124 (2011) 2338-2349.
8. J. Matsubara, S. Sugiyama, K. Sugamura et al., A dipeptidyl peptidase-4 inhibitor, des-fluoro-sitagliptin, improves endothelial function and reduces atherosclerotic lesion formation in apolipoprotein E-deficient mice, J. Am. Coll. Cardiol. 59 (2012) 265-276.
9. M. Kern, N. Klöting, H.G. Niessen et al., Linagliptin improves insulin sensitivity and hepatic steatosis in diet-induced obesity, PLoS One 7 (2012) e38744.
10. T. Klein, M. Fujii, J. Sandel et al., Linagliptin alleviates hepatic steatosis and inflammation in a mouse model of non-alcoholic steatohepatitis, Med. Mol. Morphol. 47 (2014) 137-149.
11. M.R. Dweck, E. Aikawa, D.E. Newby et al., Noninvasive molecular imaging of disease activity in atherosclerosis, Circ. Res. 119 (2016) 330–340.
12. T.N. Kim, S. Kim, S.J. Yang et al., Vascular inflammation in patients with impaired glucose tolerance and type 2 diabetes: analysis with $^{18}$F-fluorodeoxyglucose positron emission tomography, Circ. Cardiovasc. Imaging 3 (2010) 142-148.
13. J. Bucerius, V. Mani, C. Moncrieff et al., Impact of noninsulin-dependent type 2 diabetes on carotid wall $^{18}$F-fluorodeoxyglucose positron emission tomography uptake, J. Am. Coll. Cardiol. 59 (2012) 2080-2088.
14. SJ. Yang, S. Kim, SY. Hwang et al., Association between sRAGE, esRAGE levels and vascular inflammation: analysis with (18)F-fluorodeoxyglucose positron emission tomography. Atherosclerosis. 220 (2012) 402-406.

15. N. Tahara, H. Kai, S. Yamagishi et al., Vascular inflammation evaluated by [$^{18}$F]-fluorodeoxyglucose positron emission tomography is associated with the metabolic syndrome, J. Am. Coll. Cardiol. 49 (2007) 1533-1539.
16. L. Tomas, A. Edsfeldt, IG. Mollet et al., Altered metabolism distinguishes high-risk from stable carotid atherosclerotic plaques. Eur. Heart J. 39 (2018) 2301-2310.
17. S.E. Heinonen, P. Leppänen, I. Kholová et al., Increased atherosclerotic lesion calcification in a novel mouse model combining insulin resistance, hyperglycemia, and hypercholesterolemia, Circ. Res. 101 (2007) 1058-1067.
18. V. Darsalia, M. Larsson, G. Lietzau et al., Gliptin-mediated neuroprotection against stroke requires chronic pretreatment and is independent of glucagon-like peptide-1 receptor, Diabetes Obes. Metab. 18 (2016) 537-541.
19. J.M. Silvola, A. Saraste, I. Laitinen et al., Effects of age, diet, and type 2 diabetes on the development and FDG uptake of atherosclerotic plaques, JACC Cardiovasc. Imaging 4 (2011) 1294-1301.
20. M. Hjelkrem, C. Stauch, J. Shaw, S.A. Harrison, Validation of the non-alcoholic fatty liver disease activity score, Aliment Pharmacol. Ther. 34 (2011) 214-218.
21. P. Rinne, J.M. Silvola, S. Hellberg et al., Pharmacological activation of the melanocortin system limits plaque inflammation and ameliorates vascular dysfunction in atherosclerotic mice, Arterioscler. Thromb. Vasc. Biol. 34 (2014) 1346-1354.
22. M. Arakawa, T. Mita, K. Azuma et al., H. Inhibition of monocyte adhesion to endothelial cells and attenuation of atherosclerotic lesion by a glucagon-like peptide-1 receptor agonist, exendin-4, Diabetes 59 (2010) 1030-1037.
23. T. Gaspari, I. Welungoda, R.E. Widdop, R.W. Simpson, A.E. Dear, The GLP-1 receptor agonist liraglutide inhibits progression of vascular disease via effects on atherogenesis, plaque stability

and endothelial function in an ApoE(-/-) mouse model, Diab. Vasc. Dis. Res. 10 (2013) 353-360.

24. N. Panjwani, E.E. Mulvihill, C. Lonquet et al., GLP-1 receptor activation indirectly reduces hepatic lipid accumulation but does not attenuate development of atherosclerosis in diabetic male ApoE(-/-) mice, Endocrinology 154 (2013) 127-139.
25. F.M. van der Valk, S.L. Verweij, K.A. Zwinderman et al., Thresholds for arterial wall inflammation quantified by $^{18}$F-FDG PET imaging: Implications for vascular interventional studies, JACC Cardiovasc. Imaging 9 (2016) 1198–1207.
26. S. Hellberg, S. Sippola, H. Liljenbäck et al., Effects of atorvastatin and diet interventions on atherosclerotic plaque inflammation and [$^{18}$F]FDG uptake in Ldlr$^{-/-}$Apob$^{100/100}$ mice. Atherosclerosis 263 (2017) 369-376.
27. F. Zhuge, Y. Ni, M. Nagashimada et al., DPP-4 inhibition by linagliptin attenuates obesity-related inflammation and insulin resistance by regulating M1/M2 macrophage polarization, Diabetes 65 (2016) 2966-2979.
28. A.D. Dobrian, Q. Ma, J.W. Lindsay et al., Dipeptidyl peptidase IV inhibitor sitagliptin reduces local inflammation in adipose tissue and in pancreatic islets of obese mice, Am. J. Physiol. Endocrinol. Metab. 300 (2011) E410-421.
29. L.J. Carbone, P.W. Angus, N.D. Yeomans, Incretin-based therapies for the treatment of non-alcoholic fatty liver disease: A systematic review and meta-analysis, J. Gastroenterol. Hepatol. 31 (2016) 23-31.
30. S.V. Michurina, I.J. Ishenko, V.V. Klimotov et al., Linagliptin alleviates fatty liver disease in diabetic *db/db* mice, World J. Diabetes 7 (2016) 534-546.
31. G. Keramida, J. Potts, J. Bush et al., Accumulation of $^{18}$F-FDG in the liver in hepatic steatosis. AJR Am. J. Roentgenol. 203 (2014) 643-648. Erratum in: AJR Am. J. Roentgenol. 204 (2015) 1137.

32. S.P. Hong, T.S. Noh, S.H. Moon et al., Hepatic glucose uptake is increased in association with elevated serum γ-glutamyl transpeptidase and triglyceride, Dig. Dis. Sci. 59 (2014) 607-613.
33. S.H. Moon, S.P. Hong, Y.S. Cho et al., Hepatic FDG uptake is associated with future cardiovascular events in asymptomatic individuals with non-alcoholic fatty liver disease, J. Nucl. Cardiol. 24 (2017) 892-899.
34. C. Buettner, J.H. Rudd, Z.A. Fayad, Determinants of FDG uptake in atherosclerosis, JACC Cardiovasc. Imaging 4 (2011) 1302-1304.

**Table 1.** Characteristics of the study mice.

| | | | | | | |
|---|---|---|---|---|---|---|
| | | | | | *p*-value | *p*-value |
| | | | | | Linagliptin | Linagliptin *vs.* HFD |
| | | | | | HFD | |
| | | | | | Chow | |

HFD *vs.* Chow

| | | | | | | |
|---|---|---|---|---|---|---|
| | n | 15 | 14 | 5 | | |
| Baseline | Body mass (g) | 33 ± 3.0 | 34 ± 1.8 | 31 ± 3.1 | 0.33 | 0.05 |
| | Fasting glucose (mmol/l) | 9.8 ± 1.5 | 9.6 ± 3.0 | 11 ± 1.5 | 0.77 | 0.39 |
| | Fasting insulin (ng/ml) | 0.56 ± 0.18 | 0.60 ± 0.27 | ND | 0.69 | |
| | Total cholesterol (mmol/l) | 35 ± 8.3 | 35 ± 14 | 8.0 ± 3.2 | 0.99 | <0.001 |
| | Triglycerides (mmol/l) | 2.5 ± 0.83 | 2.3 ± 0.54 | 2.2 ± 0.43 | 0.30 | 0.72 |
| End of study | Body mass (g) | 35 ± 2.9 | 36 ± 3.1 | 33 ± 4.4 | 0.25 | 0.09 |
| | Liver mass (mg) | 2,018 ± 486 | 2,117 ± 449 | 1,617 ± 255 | 0.59 | 0.03 |
| | Fasting glucose (mmol/l) | 9.3 ± 1.5 | 10.3 ± 2.5 | 9.0 ± 1.2 | 0.19 | 0.27 |
| | Fasting insulin (ng/ml) | 0.44 ± 0.15 | 0.53 ± 0.25 | ND | 0.29 | |
| | Total cholesterol (mmol/l) | 31 ± 14 | 33 ± 12 | 8.6 ± 1.7 | 0.73 | <0.001 |
| | Triglycerides (mmol/l) | 2.0 ± 0.88 | 2.4 ± 0.70 | 1.8 ± 0.10 | 0.26 | 0.08 |

HFD, high-fat diet; ND, not determined. Values are mean ± SD and *p*-values from Student's *t*-test.

**Table 2.** Quantitative results of the $^{18}$F-FDG autoradiography, histology, and immunohistochemistry.

| | Linagliptin ($n$ = 15) | HFD ($n$ = 14) | Chow ($n$ = 5) | $p$-value Linagliptin *vs.* HFD | $p$-value HFD *vs.* Chow |
|---|---|---|---|---|---|
| **$^{18}$F-FDG autoradiography** | | | | | |
| Aorta | | | | | |
| Adventitia (PSL/mm$^2$) | 95 ± 27 | 88 ± 18 | 103 ± 56 | 0.45 | 0.36 |
| Wall (PSL/mm$^2$) | 116 ± 33 | 114 ± 24 | 127 ± 75 | 0.81 | 0.54 |
| Plaque (PSL/mm$^2$) | 197 ± 54 | 182 ± 40 | 217 ± 136 | 0.41 | 0.38 |
| Plaque-to-wall ratio | 1.7 ± 0.25 | 1.6 ± 0.21 | 1.7 ± 0.19 | 0.24 | 0.39 |
| Liver (PSL/mm$^2$) | 116 ± 29 | 134 ± 36 | 93 ± 16 | 0.17 | 0.03 |
| **Aortic root histology and immunohistochemistry** | | | | | |
| Mac-3-positive area (%) | 12 ± 2.2 | 12 ± 1.9 | 13 ± 0.8 | 0.70 | 0.11 |
| iNOS-positive area (%) | 6.3 ± 2.8 | 4.4 ± 1.9 | 4.8 ± 2.2 | 0.06 | 0.76 |
| MRC-1-positive area (%) | 16 ± 3.6 | 16 ± 3.9 | 17 ± 3.5 | 0.89 | 0.64 |
| MRC-1/iNOS ratio | 3.6 ± 2.9 | 4.5 ± 2.3 | 5.1 ± 4.2 | 0.37 | 0.69 |
| Area of the intima (mm$^2$) | 0.87 ± 0.22 | 0.99 ± 0.34 | 0.24 ± 0.15 | 0.26 | <0.001 |
| Intima-to-media ratio | 4.0 ± 1.2 | 4.8 ± 2.4 | 0.9 ± 0.64 | 0.24 | 0.002 |
| **Liver histopathology** | | | | | |
| Steatosis | 2.0 ± 1.1 | 2.3 ± 1.0 | 0.80 ± 0.45 | 0.85 | 0.02 |
| Inflammation | 0.93 ± 0.59 | 1.4 ± 1.3 | 0.80 ± 0.84 | 0.04 | 0.69 |
| Hepatocellular ballooning | 1.1 ± 0.59 | 1.2 ± 0.70 | 0.80 ± 0.45 | 0.68 | 0.36 |
| NAS | 4.0 ± 1.4 | 4.9 ± 1.6 | 2.8 ± 1.9 | 0.37 | 0.29 |
| Fibrosis | 0.40 ± 0.51 | 0.71 ± 0.83 | 0.00 ± 0.00 | 0.57 | 0.14 |

$^{18}$F-FDG, 2-deoxy-2-[$^{18}$F]-fluoro-*D*-glucose; HFD, high-fat diet;; iNOS, inducible nitric oxide synthase; Mac-3, macrophages immunopositive for the Mac-3 antibody; MRC-1, mannose-receptor C-type 1; NAS, NAFLD activity score; PSL/mm$^2$, photo-stimulated luminescence per square millimeter. Values are mean ± SD and $p$-values in autoradiography and aortic root histology from Student's $t$-test and in liver histopathology from Fisher´s exact test.

**Figure legends**

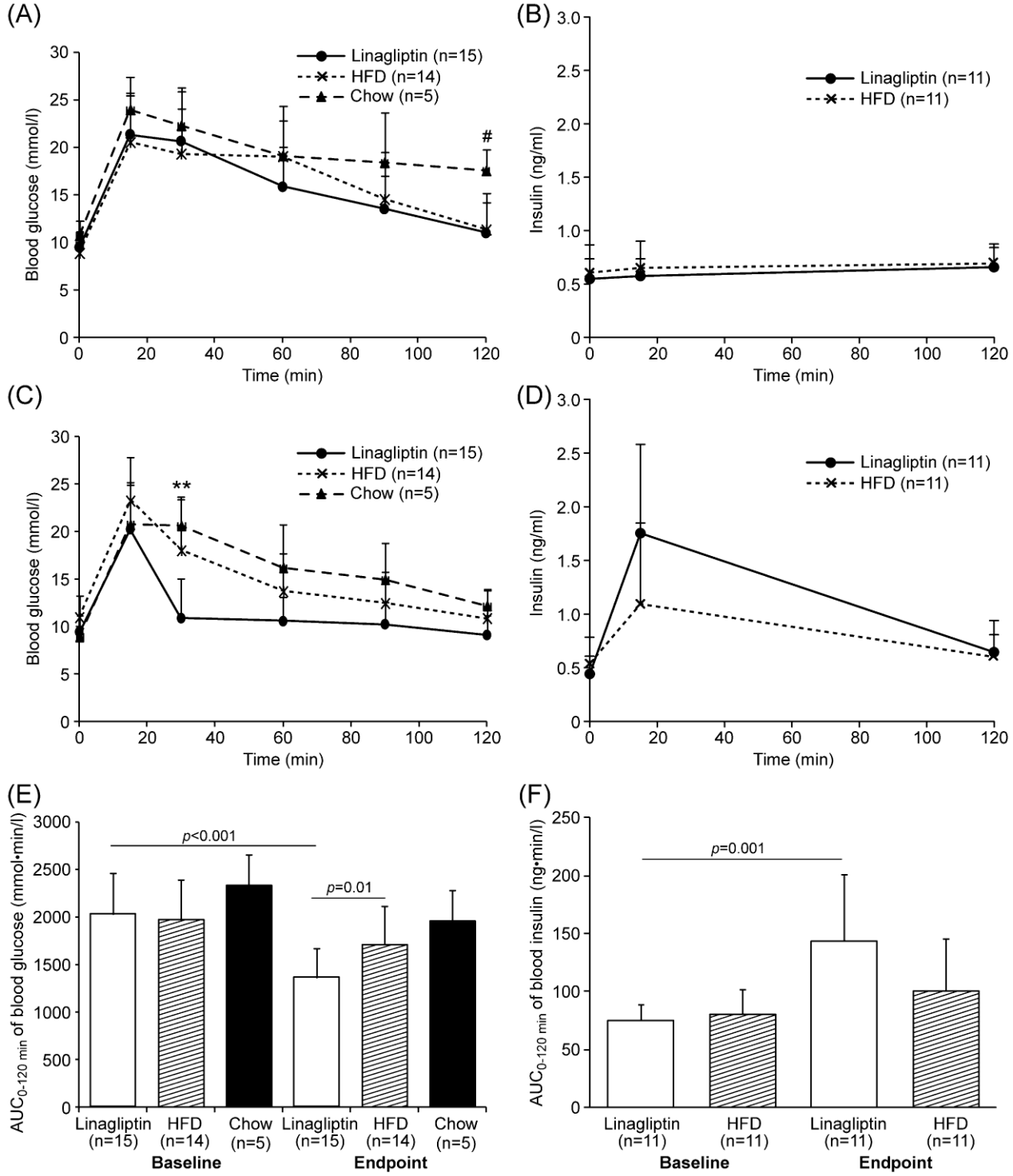


**Fig. 1. Oral glucose tolerance testing.**

(A) Baseline glucose, (B) baseline insulin, (C) endpoint glucose, (D) endpoint insulin, and (E) area under the curve of blood glucose and (F) blood insulin at baseline and the endpoint. Values are mean

± SD and *p*-values from Student's *t*-test. # HFD *vs.* chow $p < 0.01$; ** Linagliptin *vs.* HFD $p < 0.001$. n=number

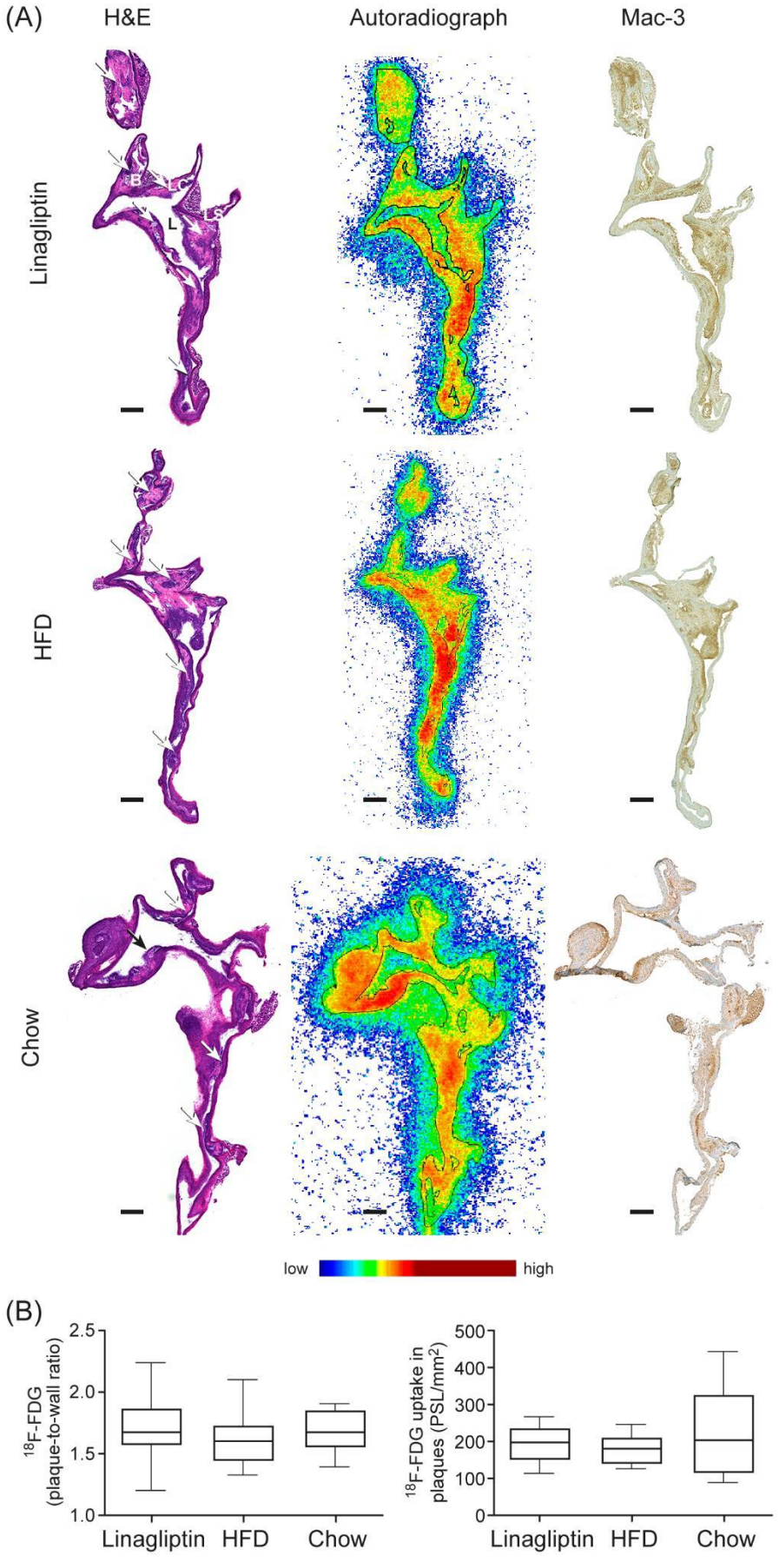
(A)
H&E
Autoradiograph
Mac-3
Linagliptin
HFD
Chow
B
LC
LS
L
low
high
(B)
18F-FDG (plaque-to-wall ratio)
2.5
2.0
1.5
1.0
Linagliptin
HFD
Chow
18F-FDG uptake in plaques (PSL/mm2)
500
400
300
200
100
0
Linagliptin
HFD
Chow

**Fig. 2. $^{18}$F-FDG autoradiography of the aortic arch.**

(A) Representative longitudinal aortic tissue sections from linagliptin-treated, HFD and chow fed mouse (scale bar: 500 µm). Left panel: hematoxylin-eosin staining showed that mice in all groups had atherosclerotic plaques (arrows). L = lumen; B = brachiocephalic artery; LC = left common carotid artery; LS = left subclavian artery. Middle panel: autoradiography shows $^{18}$F-FDG uptake in the plaques. Right panel: plaques show Mac-3 positive macrophages. (B) Quantitative results of $^{18}$F- FDG uptake (mean ± SD). Statistical analysis was performed using Student's *t*-test. n=number

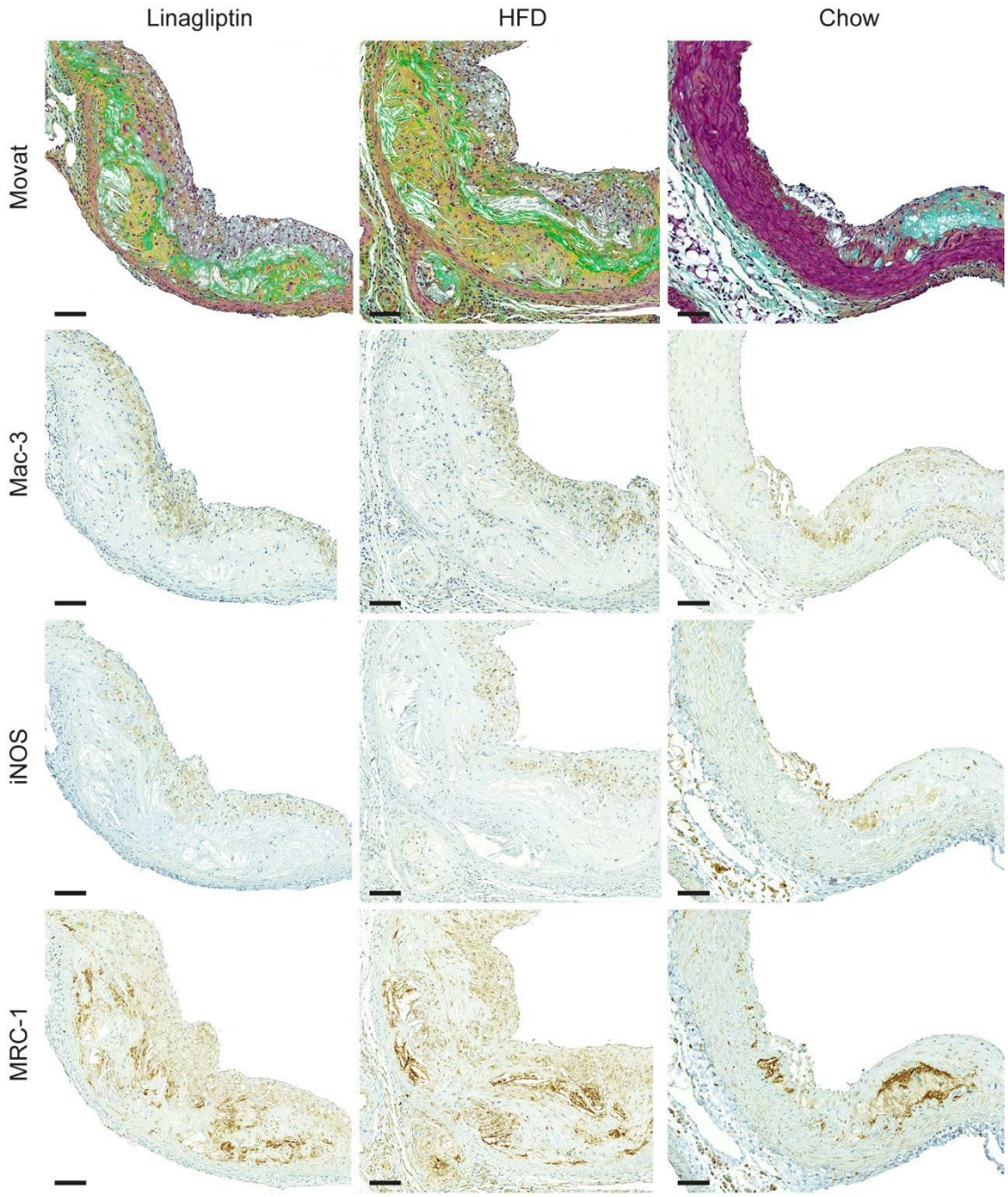


**Fig. 3. Aortic root histology and immunohistochemistry.**

Representative transverse aortic tissue sections at the level of the aortic sinus from a linagliptin-treated, HFD and chow fed mouse (scale bar: 100 µm). The sections were stained with anti-Mac-3 antibody (for macrophages), anti-inducible nitric oxide synthase (iNOS) antibody (for M1-polarized macrophages), anti-mannose-receptor C-type 1 (MRC-1) (for M2 polarized macrophages), and Movat's pentachrome (for histologic assessment).

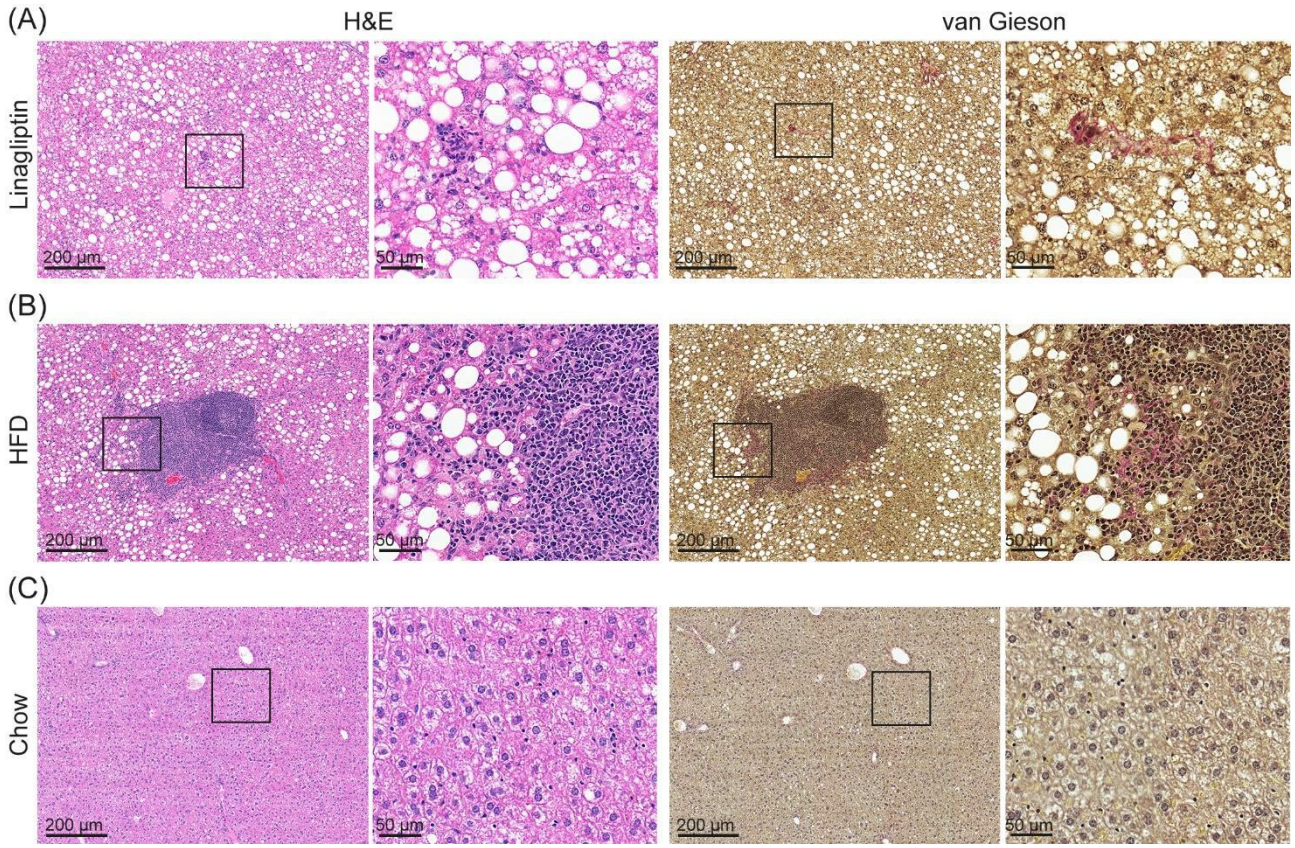


**Fig. 4. Liver histopathology.**

Representative longitudinal liver tissue sections from (A) a mouse treated with linagliptin, (B) a HFD mouse and (C) chow fed mouse. The sections were stained with hematoxylin and eosin (H&E; left panel) and van Gieson's stain (right panel).

**Supplemental data**

# Effects of dipeptidyl peptidase 4 inhibition on inflammation in atherosclerosis: A $^{18}$F-fluorodeoxyglucose study of a mouse model of atherosclerosis and type 2 diabetes

Jenni Virta[a], Sanna Hellberg[a,b], Heidi Liljenbäck[a,c], Mia Ståhle[a], Johanna M. U. Silvola[a], Jenni Huusko[d], Mirva Söderström[e], Juhani Knuuti[a,f], Pirjo Nuutila[a,f,g], Seppo Ylä-Herttuala[d,h], Maria F. Gomez[i], Anne Roivainen[a,c,f], Antti Saraste[a,f,j]

[a]Turku PET Centre, University of Turku, Kiinamyllynkatu 4-8, FI-20520 Turku, Finland

[b]Department of Medicine, Karolinska Institutet, Akademiska stråket 1, SE-17164 Solna, Sweden

[c]Turku Center for Disease Modeling, University of Turku, Kiinamyllynkatu 10, FI-20520 Turku, Finland

[d]A.I. Virtanen Institute for Molecular Sciences, University of Eastern Finland, Kuopio, Neulanniementie 2, FI-70210 Kuopio, Finland

[e]Department of Pathology, Turku University Hospital, Kiinamyllynkatu 10, FI-20520 Turku, Finland

[f]Turku PET Centre, Turku University Hospital, Kiinamyllynkatu 4-8, FI-20520 Turku, Finland

[g]Department of Endocrinology, Turku University Hospital, Kiinamyllynkatu 4-6, FI-20520 Turku, Finland

[h]Heart Center, Kuopio University Hospital, Puijonlaaksontie 2, FI-70210 Kuopio, Finland

[i]Department of Clinical Sciences, Lund University, Jan Waldenströms gata 35, SE-21428 Malmö, Sweden

[j]Heart Center, Turku University Hospital, Hämeentie 11, FI-20520 Turku, Finland

*Metabolic analyses and plasma biomarkers*

The mice were fasted for 5 h prior to oGTT. All the mice were administered a fixed dose of glucose (180 µl of 20% glucose) *per os*, and glucose was measured using a glucometer (Contour Next, Bayer AG, Leverkusen, Germany) in tail vein blood before (0 min) and 15, 30, 60, 90, and 120 min after the administration of glucose. Blood insulin concentration was measured in 11 mice from linagliptin and HFD group before and 15 and 120 min after glucose administration, using an enzyme-linked immunosorbent assay (Ultra-sensitive Mouse Insulin ELISA Kit; Crystal Chem, Chicago, IL, USA).

Plasma total cholesterol and triglyceride concentrations were measured at baseline and at the end of the intervention. Cholesterol measurements were performed using a Cholesterol ChOD-PAP kit (MTI-diagnostics GmbH, Idstein, Germany) and triglycerides using a Triglyceride Determination Kit (Sigma-Aldrich, St. Louis, MO, USA).

*Immunohistochemistry of the aortic root*

Antibodies used in the assessment of macrophage infiltration and polarization in the aortic root were as follows: mouse anti-Mac-3 (anti-Mac-3 clone M3/84, 1:500; BD Biosciences, Franklin Lakes, NJ, USA); anti-mannose receptor C-type 1 antibody (MRC-1) and anti-inducible nitric oxide synthase antibody (iNOS) (anti-MRC-1 ab64693, 1:500 and anti-iNOS ab15323, 1:200; Abcam, Cambridge, UK).

*Histologic assessment of the liver*

Liver histology was evaluated and scored for the severity of non-alcoholic fatty liver disease (NAFLD) using 4 µm sections stained with hematoxylin and eosin (H&E) or van Gieson's stain. Hepatic steatosis was scored as 0 (>5% steatosis), 1 (5–33% steatosis), 2 (34–66% steatosis), or 3

(>66% steatosis). The number of inflammatory foci per field of view were counted in five different fields at ×100 magnification (area: 3.1 $mm^2$) and scored as 0 (<0.5 foci), 1 (0.5–1.0 foci), 2 (1.0–2.0 foci), or 3 (>2 foci). Hepatocellular ballooning was scored as 0 (no ballooning), 1 (a few ballooned cells), or 2 (many ballooned cells or prominent ballooning). The NAFLD activity score was calculated by adding the scores for steatosis, ballooning, and inflammation (all equally weighted). Fibrosis was assessed on van Gieson's-stained sections and scored as 0 (no fibrosis), 1 (lobular reticular fibrosis), 2 (portal), 3 (bridging fibrosis), or 4 (cirrhosis).

**Supplemental Table 1.** *Ex vivo* biodistribution of $^{18}$F-FDG radioactivity 90 min post-injection in linagliptin, HFD and chow groups.

| Tissue | Linagliptin (n=15) | HFD (n=14) | Chow (n=5) | *p*-value Linagliptin *vs.* HFD | *p*-value HFD *vs.* Chow |
|---|---|---|---|---|---|
| Aorta | 1.04 ± 0.23 | 1.07 ± 0.27 | 1.2 ± 0.58 | 0.74 | 0.54 |
| Blood | 0.33 ± 0.04 | 0.36 ± 0.07 | 0.47 ± 0.15 | 0.26 | 0.03 |
| Plasma | 0.32 ± 0.05 | 0.32 ± 0.07 | 0.38 ± 0.08 | 0.87 | 0.13 |
| Myocardium | 24 ± 7.3 | 23 ± 11 | 19 ± 7.0 | 0.69 | 0.61 |
| Liver | 0.70 ± 0.17 | 0.80 ± 0.20 | 0.64 ± 0.07 | 0.17 | 0.11 |
| Spleen | 2.4 ± 0.30 | 2.8 ± 0.71 | 2.5 ± 0.59 | 0.09 | 0.41 |
| Kidney | 1.6 ± 0.32 | 1.5 ± 0.37 | 1.8 ± 0.38 | 0.53 | 0.16 |
| Pancreas | 0.91 ± 0.20 | 0.87 ± 0.17 | 0.90 ± 0.16 | 0.58 | 0.76 |
| Lung | 2.1 ± 0.18 | 1.9 ± 0.39 | 2.4 ± 0.69 | 0.32 | 0.10 |
| Muscle | 0.40 ± 0.14 | 0.42 ± 0.20 | 0.67 ± 0.29 | 0.73 | 0.05 |
| WAT | 0.07 ± 0.02 | 0.10 ± 0.04 | 0.11 ± 0.04 | 0.04 | 0.75 |
| BAT | 1.6 ± 0.31 | 1.6 ± 0.46 | 2.6 ± 0.40 | 0.73 | 0.001 |
| Lymph node | 1.8 ± 0.41 | 1.9 ± 0.54 | 2.6 ± 0.78 | 0.57 | 0.04 |
| Brain | 1.5 ± 0.20 | 1.7 ± 0.39 | 1.7 ± 0.39 | 0.10 | 0.83 |

Results are presented as the standardized uptake values (mean ± SD) and *p*-values are from Student's *t*-test. BAT, brown adipose tissue; HFD, high-fat diet; WAT, white adipose tissue.